

## AN UPDATED DEBARCODING TOOL FOR MASS CYTOMETRY WITH CELL TYPE-SPECIFIC AND CELL SAMPLE-SPECIFIC STRINGENCY ADJUSTMENT

KRISTEN I. FREAD

*Department of Biomedical Engineering, University of Virginia,  
Charlottesville, VA 22903, USA  
Email: kif5qw@virginia.edu*

WILLIAM D. STRICKLAND

*Department of Biomedical Sciences, University of Virginia,  
Charlottesville, VA 22903, USA  
Email: wds2df@virginia.edu*

GARRY P. NOLAN

*Department of Microbiology and Immunology, Stanford University,  
Stanford, California 94305, USA  
Email: gnolan@stanford.edu*

ELI R. ZUNDER

*Department of Biomedical Engineering, University of Virginia  
Charlottesville, VA 22903, USA  
Email: ezunder@virginia.edu*

Pooled sample analysis by mass cytometry barcoding carries many advantages: reduced antibody consumption, increased sample throughput, removal of cell doublets, reduction of cross-contamination by sample carryover, and the elimination of tube-to-tube-variability in antibody staining. A single-cell debarcoding algorithm was previously developed to improve the accuracy and yield of sample deconvolution, but this method was limited to using fixed parameters for debarcoding stringency filtering, which could introduce cell-specific or sample-specific bias to cell yield in scenarios where barcode staining intensity and variance are not uniform across the pooled samples. To address this issue, we have updated the algorithm to output debarcoding parameters for every cell in the sample-assigned FCS files, which allows for visualization and analysis of these parameters via flow cytometry analysis software. This strategy can be used to detect cell type-specific and sample-specific effects on the underlying cell data that arise during the debarcoding process. An additional benefit to this strategy is the decoupling of barcode stringency filtering from the debarcoding and sample assignment process. This is accomplished by removing the stringency filters during sample assignment, and then filtering after the fact with 1- and 2-dimensional gating on the debarcoding parameters which are output with the FCS files. These data exploration strategies serve as an important quality check for barcoded mass cytometry datasets, and allow cell type and sample-specific stringency adjustment that can remove bias in cell yield introduced during the debarcoding process.

\* This work is supported in part by the University of Virginia Department of Biomedical Engineering, CIRM Basic Biology II Grant RB2-01592, and NIH F32 GM093508-01.

## 1. Introduction

### 1.1. Sample multiplexing for flow cytometry and mass cytometry with cell barcoding

Sample multiplexing, also referred to as pooled sample analysis, is a general approach that has been applied to several biological assays, including ELISA immunoassay<sup>1</sup>, next-generation DNA sequencing<sup>2,3</sup>, fluorescence-based flow cytometry<sup>4</sup>, and mass cytometry<sup>5-7</sup>. In this approach, individual samples are labeled with unique identifiers, and then pooled together for processing and measurement. These unique identifiers can be thought of as sample-specific barcodes. After processing and measurement, the pooled sample dataset is deconvolved using these barcodes to recover individual sample data for further analysis (Fig. 1A).

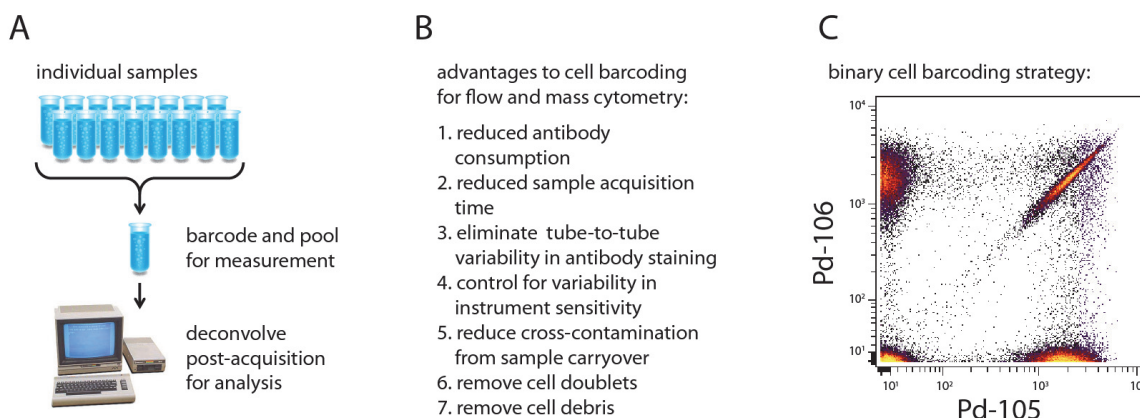


Figure 1. Mass cytometry barcoding overview. (A) General strategy for pooled sample analysis. (B) Flow and mass cytometry-specific advantages to cell barcoding for pooled sample analysis. (C) Binary cell barcoding strategy for flow and mass cytometry, in which every cell is labeled either positively or negatively on barcode-dedicated channels.

The obvious advantages gained by sample multiplexing are a) reducing the time and resources required to analyze multiple samples, and b) improving the comparability between samples, because they are processed identically after pooling. Major advantages specific to flow cytometry and mass cytometry include reduced antibody consumption, increased sample acquisition rate, and the elimination of tube-to-tube variability in antibody staining conditions (Fig. 1B).

Sample multiplexing for fluorescence-based flow cytometry is performed with cell-reactive dyes that bind irreversibly to accessible nucleophiles on the cell<sup>4</sup>. These accessible nucleophiles include free thiols present on cysteine residues, and free amines present on lysine residues and at the N-terminus of proteins. While not strictly required, cell permeabilization greatly improves cell barcoding performance by increasing the number of accessible nucleophiles available on each cell. Multiple levels of fluorophore labeling can be achieved – previous studies have demonstrated 96-sample multiplexing with only 3 dedicated fluorescence channels: Alexa Fluor 700 (4 staining levels), Pacific Blue (4 staining levels), and Alexa Fluor 488 (6 staining levels)<sup>4</sup>. This multi-level

staining approach allows for a high level of multiplexing with limited measurement channels, but relies on uniform levels of dye reactivity between all cell types and samples.

If there is considerable variability in labeling reagent uptake between cell types or sample types, a simpler binary cell barcoding approach can be applied to improve the fidelity of cell sample assignment at the deconvolution step. Because each cell sample is labeled either positively or negatively on each barcode-dedicated channel, the two populations are better separated with less potential for overlap (Fig. 1C). This approach is favored for mass cytometry cell barcoding, because the lanthanide and palladium-based barcode reagents react rapidly with cells even at 4°C<sup>5,7</sup>, making the labeling reaction effectively stoichiometric and therefore more sensitive to variability between the samples in cell number, cell type/size, the presence of cellular debris, and residual bovine serum albumin (BSA) from the wash buffer. Using a binary barcode scheme requires more barcode-dedicated measurement channels than multi-level labeling, but allows for greater sample assignment fidelity during deconvolution while still permitting over 40 molecular measurements per cell with a staining panel made up of lanthanide-based mass cytometry antibodies, I127-IdU to mark S-phase cells<sup>8</sup>, and cisplatin as a viability stain<sup>9</sup>.

### **1.2. Doublet-filtering cell barcode scheme**

Cell doublets (as well as triplets, quadruplets, and higher-order cell clusters) pose a significant challenge for single-cell analysis. When analyzing or performing fluorescence-activated cell sorting (FACS) on cell samples with known and well-defined cell types, such as whole blood or primary blood mononuclear cells (PBMCs), cell doublets are for the most part an annoyance that can be gated out using cell surface markers and light scatter properties. In certain defined settings, the study of cell doublets by flow cytometry has even proved to be illuminating with respect to cell adhesion and cell-cell interactions<sup>10</sup>. However, during exploratory analysis of uncharacterized cell samples and cell types, cell doublets are especially problematic, because they may be falsely interpreted as a novel cell type that shares the molecular characteristics of its two component cells.

Fluorescence-based flow cytometry has forward scatter (FSC) and side scatter (SSC) parameters that can be used to identify and remove cell doublets by two-dimensional gating<sup>11</sup>. Mass cytometry does not have a comparable measurement parameter, but a binary barcode scheme has been developed that can identify and remove cell doublets as well as higher-order clusters<sup>7</sup>. Instead of using every possible binary combination, this doublet-filtering barcode scheme uses a limited subset of binary combinations, such that any doublet combination will result in an “illegal” combination that is recognized as a doublet and removed from the dataset. A binary barcode scheme with  $n$  dedicated measurement channels will provide  $2^n$  unique barcode combinations, but the doublet filtering binary barcode scheme only uses  $n$ -choose- $k$  combinations, where  $k = n/2$ . 6 palladium isotopes are often used for cell barcoding because they are incompatible with the DTPA-based

polymer used to label antibodies with lanthanide metals<sup>12</sup>. Instead of multiplexing 64 samples with all binary combinations ( $2^6$ ) of the palladium isotopes, the doublet-filtering scheme only allows 20-sample multiplexing (6-choose-3) with palladium-based barcoding reagents (Fig. 2A). Because each barcode combination in this scheme is positive for exactly 3 palladium isotopes (Fig. 2B), any cell that is positive for 4 or more palladium isotopes will be identified as a cell doublet and removed from the dataset (Fig. 2C).

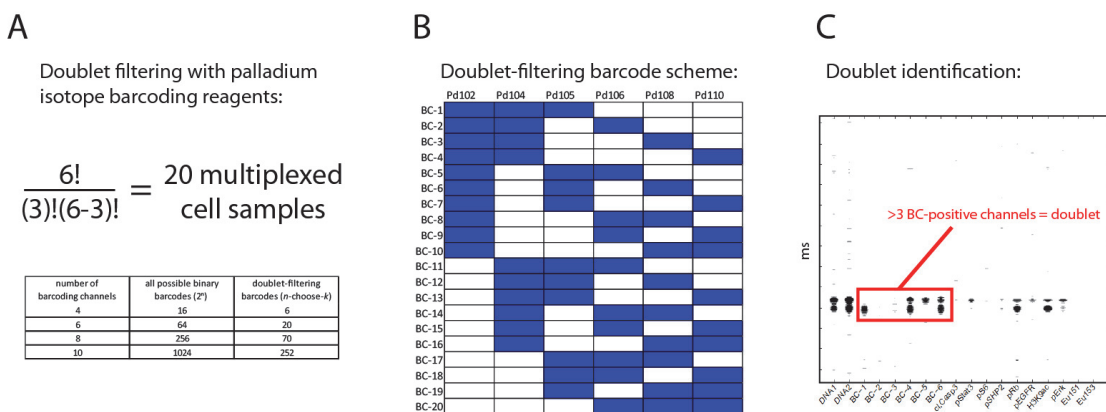


Figure 2. Doublet filtering barcode scheme. (A) Sample multiplexing with exhaustive ( $2^n$ ) and doublet-filtering ( $n$ -choose- $k$ ) barcode schemes. (B) Palladium isotope combinations for doublet-filtering barcode scheme. (C) Doublet identification by “illegal” barcode combination viewed in the mass trace scanning window of the mass cytometer.

This doublet-filtering scheme has become part of the standard mass cytometry workflow for many laboratories, and was incorporated into the third-generation Helios™ CyTOF® mass cytometer. Each user should consider the benefits of each approach for their experiment, because in some cases increased sample multiplexing could be more valuable than doublet removal. However, the recent description of ruthenium and osmium-based cell barcoding reagents suggests that high-level multiplexing with simultaneous doublet-filtering is now within reach<sup>13</sup>, without having to give up any of the traditional mass cytometry measurement channels such as the lanthanide series metals.

### 1.3. Sample deconvolution by sequential gating and Boolean gating strategies

After pooled sample analysis, sample-specific barcodes are used to recover individual sample data for analysis. Different approaches have been applied to this deconvolution step, including cell type-specific gating followed by sequential 2-D barcode gating<sup>4</sup> or Boolean 1-D barcode gating<sup>5</sup>. Two drawbacks from these gating approaches are 1) time-consuming manual gating, and 2) the potential for cell loss or sample mis-assignment. In situations where the separation between barcoded populations is not large enough to be separable (Fig. 3A), the researcher must decide whether to throw out cells that reside in this intermediate space (Fig. 3B), or to split the populations and accept

that some cells may be incorrectly assigned (Fig. 3C). In barcoded samples there is very often at least a small number of cells present in this intermediate zone that cannot be assigned to a specific sample by this debarcoding method. Usually this population is minor as shown in Figure 1C, but results like Figure 3A can also occur, particularly if the cell number in one or more samples is not estimated accurately resulting in uneven barcode labeling between samples. For this 1-D or 2-D gating strategy, boundaries can be drawn algorithmically using distribution shape and percentile cut-points, but the exact placement will depend on how the competing desires for cell yield vs. sample assignment accuracy.

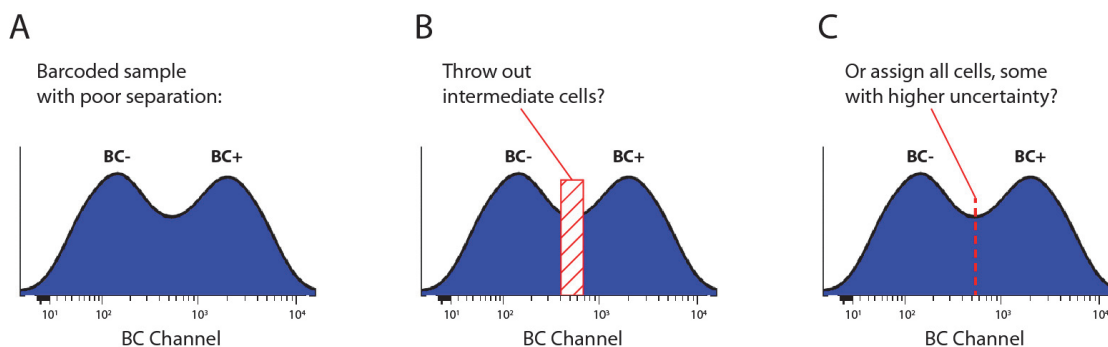


Figure 3. Traditional gating method on poorly-separated barcode sample. (A) Overlapping positive and negative barcode populations. (B) Intermediate cells can be thrown out to increase barcode deconvolution stringency. (C) Intermediate cells can be assigned to increase barcode deconvolution yield.

#### 1.4. Sample deconvolution by single-cell debarcoding algorithm

In order to recover as many cells as possible in an automated and unbiased manner, a novel method for barcode deconvolution was previously developed, termed single-cell debarcoding<sup>7</sup>. This method is designed to perform especially well with the problematic “intermediate zone” cells. Instead of population-based gating, it looks at each cell individually, and asks “which sample barcode does this cell most closely resemble?” Sample assignment and the level of confidence associated with it is calculated by the separation distance between normalized positive and negative barcode channel measurements (Fig. 4A). The choice of separation distance used for this calculation depends on the binary barcode scheme being used. For exhaustive non-doublet-filtering barcode schemes, the largest separation distance is identified. For doublet-filtering barcode schemes, the distance between the top  $n/2$  and bottom  $n/2$  normalized barcode intensities is used, whether or not this is the largest separation distance present. If the separation distance is large, there is high confidence that the barcode sample assignment is correct. If the separation distance is small, there is low confidence that the barcode sample assignment is correct and these cells may be discarded depending on the deconvolution stringency desired.

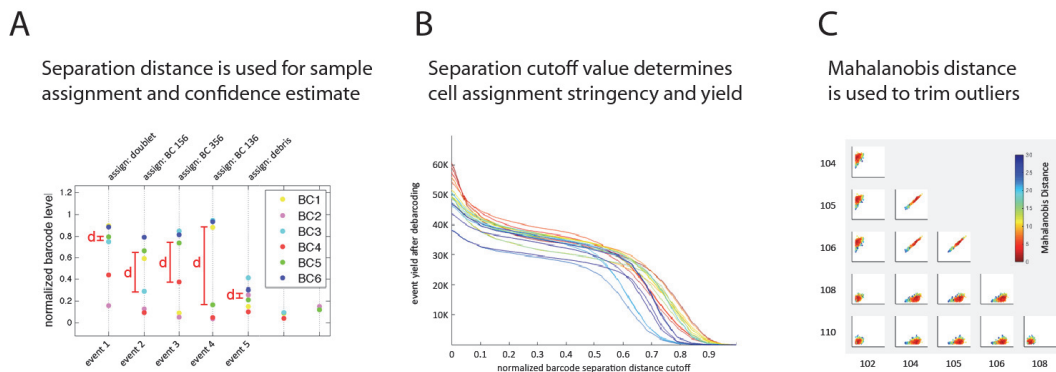


Figure 4. Single-cell debarcoding algorithm. (A) After normalization of the individual barcode channel intensities, separation distances (indicated by a red line and the letter “d”) are calculated for every cell. In this example, a 6-channel doublet-filtering barcode scheme was used. Therefore, event 1 does not receive a sample assignment because it appears to be a doublet with 4 positive barcode channels and a small separation distance between the top 3 and bottom 3 barcode intensities. Event 5 has low normalized intensities for all 6 barcode measurement channels, and therefore appears to be “debris.” (B) The relationship between separation distance cutoff and debarcoder cell yield. Each colored line represents one of the 20 samples in a 6-metal, doublet-filtering, pooled sample dataset. Cell yield decreases with increasing separation distance cutoff stringency, but plateaus somewhat between 0.1 and 0.6. (C) Mahalanobis plots of every barcode-by-barcode biaxial plot for a single assigned cell sample. Every cell is colored by mahalanobis distance, from low (0-red) to high (30-blue).

The single-cell debarcoding software tool was released as a MATLAB standalone executable (<https://github.com/nolanlab/single-cell-debarcoder>)<sup>7</sup> that does not require a MATLAB installation (<http://www.mathworks.com/products/compiler/>). This software tool performs debarcoding and sample assignment in a semi-automated manner, presenting the user with visualizations that aid in the choice of two key debarcoding parameters: the separation distance cutoff which affects sample assignment stringency and cell yield (Fig. 4B), and the mahalanobis distance cutoff which is used to trim outliers (Fig. 4C). Standard practice for the single-cell debarcoder is to choose a separation cutoff distance that is as stringent as possible without severe cell loss, such as approximately 0.5 in Figure 4B. Most separation distance plots follow a similar trend, with a plateau in the center flanked by steep declines in the 0-0.1 range (debris and cell doublets) and approaching 1 (all cells will eventually fail the stringency test). Mahalanobis plots are more variable, depending on the mix of cell types in each sample. There is no specific rule or recommendation for setting the mahalanobis distance cutoff, but the default setting of 30 is a good starting point for 6-metal/20-sample palladium-barcoded samples. After the user selects values for the separation distance cutoff and mahalanobis distance cutoff parameters, the single-cell debarcoder tool outputs every deconvolved cell sample as an FCS file.

### 1.5 Limitations and drawbacks to using fixed-value debarcoding cutoff parameters

Applying the same parameter cutoffs to each sample while debarcoding as previously described<sup>7</sup> is not optimal, because each sample was barcode-stained individually and will therefore vary in barcode staining intensity and population-level variance. If all samples are similar (in terms of cell type, cell number, cellular debris, and residual BSA concentration) and the cell barcoding protocol is performed precisely, then barcode staining will be fairly uniform across every sample. Frequently this is not the case however, resulting in considerable variability of barcode staining between cell samples and large differences in sample behavior with respect to the debarcoding parameters, especially the normalized barcode separation distance cutoff (Fig. 5A).

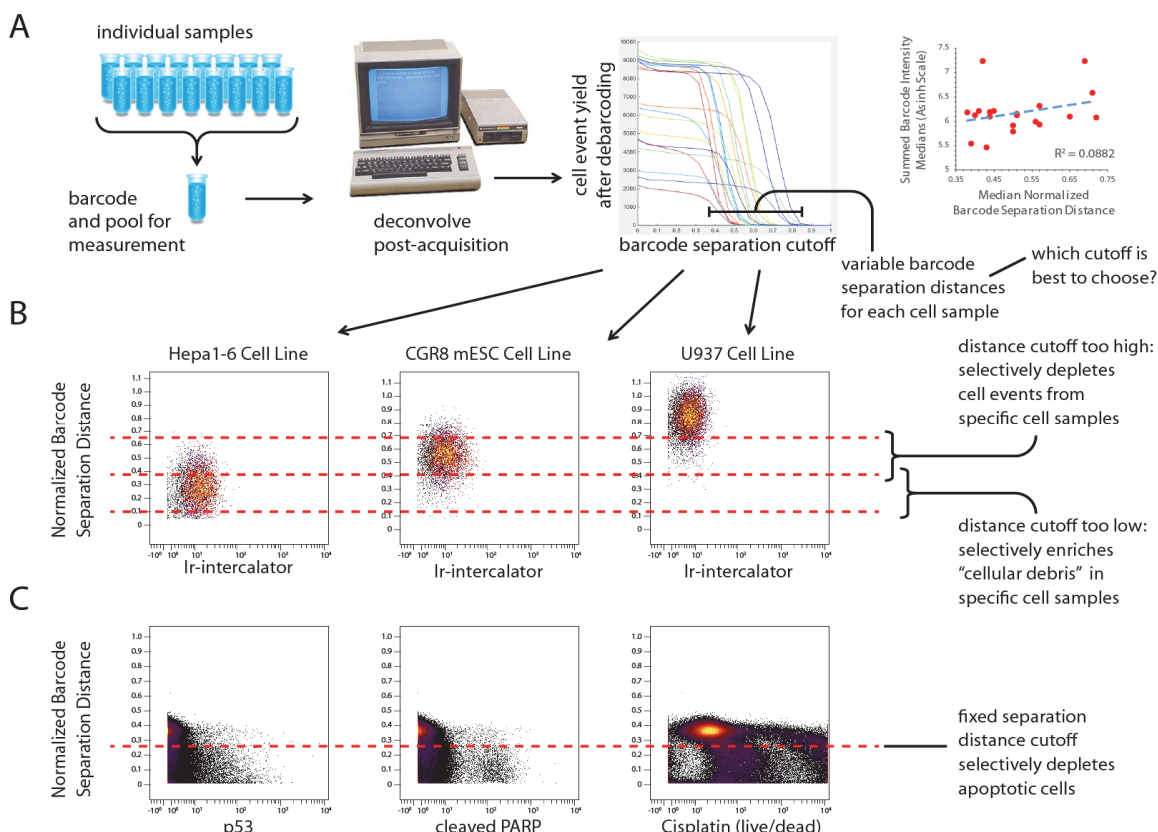


Figure 5. Cell barcode variability and its consequences. (A) Cell samples representing 20 different cell types were barcoded by the 6-palladium doublet-filtering method and then pooled for analysis. The amount of barcode reagent added to each sample was adjusted according to cell number in each sample to normalize barcode staining intensity. Variability in barcode separation distance was observed between the samples, but is only weakly correlated to barcode staining intensity, as measured by the 6-metal summed barcode intensity medians for each sample. (B) Three of the twenty barcoded cell samples, which show highly variable barcode separation distance levels, precluding a single optimal cutoff value. (C) Apoptotic cells with elevated levels of p53, cleaved-PARP, and cisplatin labeling have reduced barcode separation distance, and could be unintentionally discarded from analysis with a typical debarcoding workflow.

In this scenario, no single cutoff value for barcode separation distance is optimal for every sample, forcing the researcher to choose between depleting cells of interest in some samples, or enriching for cellular debris in other samples (Fig. 5B). In addition to cross-sample differences, different cell types can be depleted or enriched within a single sample due to differences in barcode staining behavior based on cell size, cell identity, or cell state (Fig. 5C). These sample-specific and cell type-specific effects are usually minimal, but have the potential to introduce bias into the analysis and conclusions drawn from barcoded mass cytometry experiments. Therefore, each barcoded dataset should be investigated to detect the extent of these effects, and correct for them if necessary.

## 2. Methods

### 2.1 Output single-cell debarcoding parameters with each FCS file for visualization and analysis

With the previously released debarcoding tool<sup>7</sup>, investigating the possibility for barcode-related enrichment or depletion of specific samples and cell types required laborious and time-consuming back and forth between rounds of debarcoding and FCS file analysis. Side-by-side comparison of FCS files debarcoded with iterative values for the debarcoding parameters was necessary to detect cell type or sample-specific effects. To obviate the need for this slow and inefficient analysis, we have updated the debarcoding software tool to output the debarcoding parameter values for each cell as additional data columns in the FCS file. This update allows for visualization of the barcode parameters, and analysis of how they interact with the other measured parameters and cell types of interest. The MATLAB source code for the updated software tool as well as pre-compiled executable files that do not require MATLAB installation are available to download at <https://github.com/zunderlab/single-cell-debarcoder>.

### 2.2 Post-assignment application of debarcode stringency filter and outlier trimming

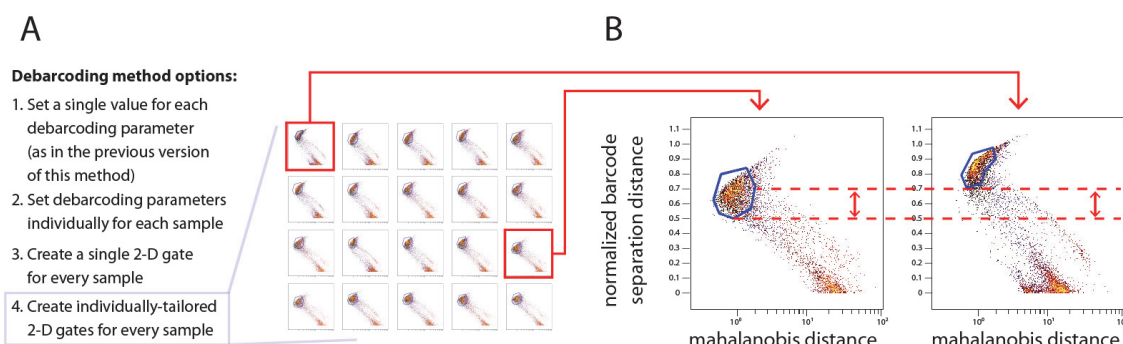


Figure 6. Sample-specific stringency adjustment by individual gating on debarcode parameters. (A) FCS output of the debarcoding parameters allows different strategies for stringency filtering. The option for individually-tailored 2-D gating on normalized barcode separation distance and mahalanobis distance is presented. (B) Two cell samples from Fig. 6A are highlighted to illustrate the population-level differences in barcode parameters between samples.

In addition to visualization and analysis, outputting the debarcode parameters in the FCS file has another practical benefit: stringency filters can be turned off during the debarcoding step and applied after the fact instead. This gives the user flexibility in their choice of stringency filtering: they may apply fixed parameters as in the previous version of this method, or perform sample-specific two-dimensional gating on the debarcode parameters (Fig. 6A). Whichever method is chosen, the user is given the tools to explore these parameters and their relationship to other cell measurements, which will aid in the choice of filtering strategy and its implementation. Some users may prefer fixed parameter stringency filtering because it is simpler and less time consuming, but users with complex, variable samples should consider individually-tailored stringency filtering, which requires more time to implement but helps prevent the introduction of sample-specific biases (Fig. 6B).

### 3. Results

#### 3.1. Precision Debarcode Stringency Filtering

The newly updated single-cell debarcoding software tool functions identically to the previous version, but with two additions: 1) values for the normalized barcode separation distance and mahalanobis distance are output for every cell, and 2) default parameters for debarcoding are set as “barcode separation threshold = 0” and “mahalanobis distance threshold = inf” (Fig. 7A). These default parameters ensure that every cell is assigned to a sample for FCS output and can be filtered after the fact. This differs from the fixed-parameter filtering which took place at the debarcoding step in the previous software version, resulting in an additional FCS output for unassigned cell events. Outputting the entire dataset (Fig. 7B) with this new method allows for precision stringency filtering by gating on the debarcode parameters (Fig. 7C). This gating will typically be performed using flow cytometry/FCS analysis software, and can be done iteratively and in combination with more fundamental cell type and dataset-specific analyses.

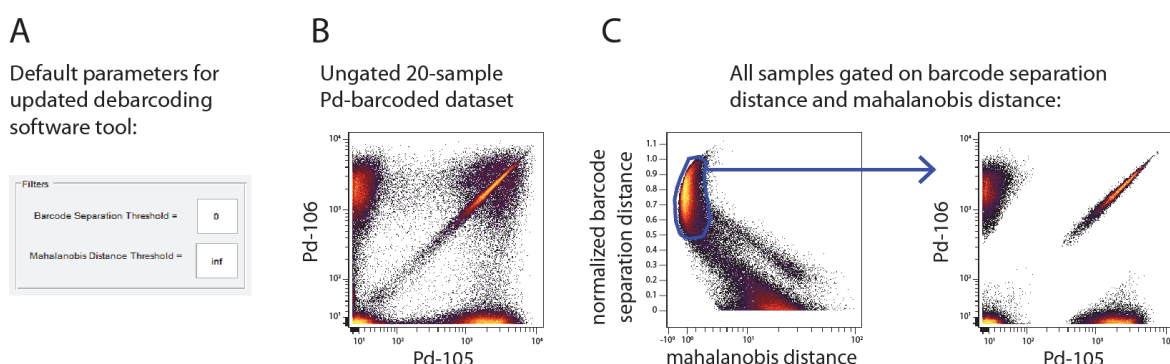


Figure 7. Debarcode stringency gating overview. (A) 20-sample Pd-based doublet-filtering barcode sample, ungated. (B) Barcode stringency trimming by 2-D gating on the normalized barcode separation distance vs. mahalanobis distance.

### 3.2 Identification and Reduction of Debarcoding-induced Sample Bias

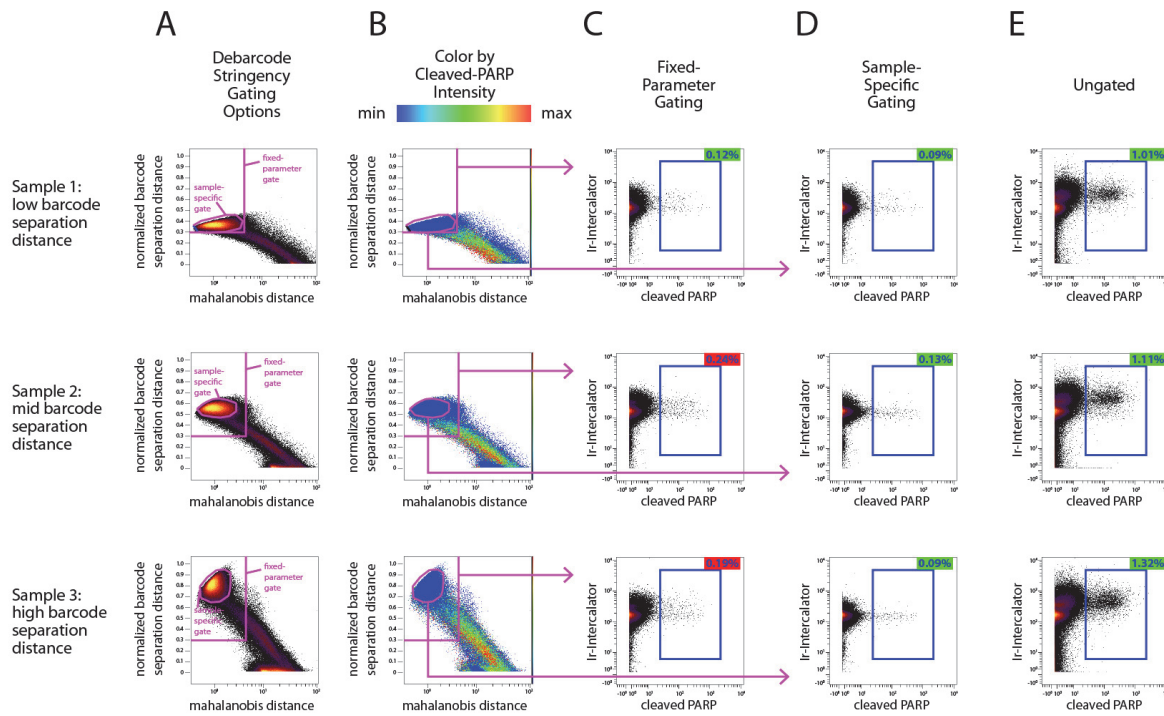


Figure 8. Sample-specific debarcode stringency gating reduces unbalanced enrichment of cleaved-PARP-positive cells. (A) Two options for stringency gating are displayed in magenta: fixed-parameter and sample-specific. (B) Cleaved-PARP intensity color scale applied to the plot from Figure 8A reveals that fewer cells with elevated cleaved-PARP levels fall within the fixed-parameter gate in sample 1 compared to samples 2 and 3. (C-E) The percentages of cleaved-PARP-positive cells present in the bulk-gated, individually-gated, and ungated populations.

Sample-specific debarcode gating on the normalized separation distance and mahalanobis parameters provides the greatest advantage over the previously used fixed-parameter debarcoding method when there is variability in the debarcode parameters between samples (Fig. 8A), which can lead to uneven distribution of specific cell types across the debarcoded samples. Cells with elevated cleaved-PARP levels are associated with lower separation distance and higher mahalanobis distance (Fig. 8B). This leads to disproportionate enrichment for cleaved-PARP cells in some samples when using fixed-parameter debarcode filtering (Fig. 8C), but is ameliorated by sample-specific gating (Fig. 8D), which more closely matches the ungated sample ratios (Fig. 8E).

### 4. Discussion

This updated method for single-cell mass cytometry debarcoding allows for visualization and analysis of the debarcoding parameters, and how they specifically relate to every other cell

measurement. This can be used to detect any cell type-specific or sample-specific effect of the debarcoding process on the underlying cell data of interest. The source code and Win/Mac executable software are available to download from <https://github.com/zunderlab/single-cell-debarcoder>. We recommend that this analysis be performed on every debarcoded dataset as a data quality check, particularly when mixed cell types and sample types are barcoded together. In addition to data quality verification, the output debarcoding parameters in every assigned FCS file can be used to guide sample-specific stringency filtering that can be performed after the fact rather than during the debarcoding process. This allows multiple stringency levels to be tested rapidly using flow cytometry/FCS analysis software, where multiple iterations of 1-D or 2-D gating can be used while monitoring the effect on cell type-specific and sample-specific cell yield as well as overall data quality. One limitation to this method is that stringency filtering is not automated, and currently relies on hand-drawn gates. While this method is optimally used to reduce cell yield and enrichment bias between cell samples and cell types that vary in barcode staining behavior, sample-specific or cell type-specific manual gating has the potential to introduce bias. As with any other hand-drawn gating analysis, the barcode gating strategy should always be presented in addition to further analysis in order to mitigate this potential for user-introduced bias. In the future, stringency filtering could be automated with sequential, percentile-based gating steps; or more complex computational methods.

### 5. Acknowledgments

This work was supported by the University of Virginia Department of Biomedical Engineering, CIRM RB2-01592, and NIH F32 GM093508-01.

### 6. References

1. Fulton et al. *Clinical Chemistry* **43**, 1749–1756 (1997).
2. Meyer et al. *Nucl. Acids Res.* **35**, e97 (2007).
3. Parameswaran et al. *Nucl. Acids Res.* **35**, e130 (2007).
4. Krutzik, P. O. & Nolan, G. P. *Nature Methods* **3**, 361–368 (2006).
5. Bodenmiller et al. *Nature Biotechnology* (2012). doi:10.1038/nbt.2317
6. Behbehani et al. *Cytometry* n/a-n/a (2014). doi:10.1002/cyto.a.22573
7. Zunder et al. *Nat. Protocols* **10**, 316–333 (2015).
8. Behbehani et al. *Cytometry Part A* **81A**, 552–566 (2012).
9. Fienberg et al. *Cytometry Part A* **81A**, 467–475 (2012).
10. Snippert et al. *Cell* **143**, 134–144 (2010).
11. Hoffman, R. A. in *Current Protocols in Cytometry* (John Wiley & Sons, Inc., 2001).
12. Majonis et al. *Biomacromolecules* **12**, 3997–4010 (2011).
13. Catena et al. *Cytometry* **89**, 491–497 (2016).